PHYSICAL REVIEW B **66**, 041201(R) (2002)

First-order pressure-induced polyamorphism in germanium

Murat Durandurdu and D. A. Drabold
Department of Physics and Astronomy, Condensed Matter and Surface Science Program, Ohio University, Athens, Ohio 45701
(Received 11 March 2002; published 16 July 2002)

We report on the pressure-induced phase transition in amorphous Germanium (a-Ge) using an *ab initio* constant pressure-relaxation simulation. a-Ge exhibits a first-order polyamorphic phase transition at 12.75 GPa with a discontinuous volume change of $\sim$19%. The transition pressure is also calculated from the Gibbs free-energy curves, and it is found that the transition occurs at 5.2 GPa in agreement, with the experimental result of 6 GPa. The pressure-induced delocalization of electronic and vibrational states is obtained.

DOI: 10.1103/PhysRevB.66.041201 PACS number(s): 64.70.Kb, 61.43.−j, 71.30.+h

Some disordered materials show an unusual response to applied pressure. H_2O (Ref. 1) undergoes a first-order phase change from a low-density amorphous phase to a high-density amorphous (HDA) phase. The existence of such multiple disordered phases is termed ''polyamorphism.'' A similar transition to that of H_2O was reported in amorphous silicon (a-Si),[2] and in SiO_2.[3,4] The general problem of disorder to disorder phase transitions in tetrahedrally bonded materials is little explored with theoretical methods because of the challenge of constructing realistic models and the lack of the good empirical potentials.

Experiment has shown that amorphous germanium (a-Ge) undergoes a transition to a metallic amorphous phase with a sharp drop in resistivity and the optical gap at room temperature around 6 GPa,[5] and it appears that this transition was first order. Minomura[6] reported that a-Ge transforms to a disordered β-Sn structure at 6–7 GPa. An amorphous to β-Sn phase transition with a 5% volume drop is seen at room temperature near 6 GPa in an x-ray diffraction study.[7] However, the amorphous sample contains some crystalline grains, and with the application of pressure the crystalline parts undergo a phase change to β-Sn (only 25% of the amorphous structure transforms to β-Sn) while the other parts still remain amorphous, a ''partial structural transition.''[7] On the other hand, no phase transition was observed up to 8.9 GPa in an EXAFS analysis of a-Ge.[8] These studies indicate that the different types of high-pressure structures can form (amorphous or crystal) depending on the sample preparation and loading condition.[7,8]

In a theoretical investigation using the Tersoff potential, a gradual amorphous to amorphous phase transformation was obtained.[9] In the same study, however, a free-energy calculation predicts a first-order amorphous to amorphous phase transition in a-Ge.[9] It is also argued that the HDA phase of a-Ge is similar to liquid-Ge (l-Ge).

Despite extensive experimental studies and one theoretical analysis, several issues concerning a-Ge under pressure remain: (1) What are the microscopic changes in the structure which occur with the application of pressure? (2) Is the transition is first order? (3) Is the transition reversible? (4) What is the nature of insulator-metal transition? In this paper, we perform accurate *ab initio* simulations of the response of a-Ge to pressure and give unambiguous answers to the issues reviewed above.

The model used here is generated using an improved version of the Wooten-Winer-Weaire algorithm.[10] At zero pressure, the model is equilibrated and relaxed with a local-orbital first-principles quantum molecular-dynamic method of Sankey and Niklewski.[11] The energy difference between diamond and the amorphous structure is found to be 150 meV/atom in agreement with 120 meV/atom from a heat crystallization measurement.[12,13] This Hamiltonian was applied to study a first-order amorphous to amorphous phase change in silicon,[2] a continuous amorphous to amorphous phase transformation in $GeSe_2$,[14] ZB$\rightarrow Cmcm \rightarrow Imm2$ transitions in GaAs,[15] and a diamond to simple hexagonal phase transition in silicon.[2] Pressure is applied via the method of Parrinello-Rahman,[16] and it is increased in increments of 2 GPa up to 12 GPa, after which an increment of 0.25 GPa is carried out in order to accurately estimate the transition pressure. Dynamical quenching at zero temperature under constant pressure is performed to fully relax the system according to the criterion that the maximum force is smaller than 0.01 eV/Å. We use Γ-point sampling for the supercells' Brillouin-zone integration, which is reasonable for a 216-atom model. A fictitious cell mass of 16×10^3 amu was found to be suitable for these simulations.

As a preliminary, we perform a simulation for crystalline Ge (c-Ge). At 22–24 GPa the diamond structure transforms into a β-Sn structure in excellent agreement with experiments. The computed transition volume ($V_t^{\beta-Sn}/V^{diamond}$) of the β-Sn is 0.65 and the axial ratio, c/a, is 0.52 at 24 GPa. Both values, however, are less than the experimental results of 0.69 and 0.551 (Ref. 17), respectively. We calculate the bulk modulus (B) and its pressure derivative (B') of diamond and β-Sn structure using the Birch-Murnaghan equation of state[18] and find $B=80$ GPa and $B'=5.19$ for diamond, which are consistent with the experimental values for diamond of $B=77$ GPa and $B'=4.6$,[19] and $B=89$ GPa and $B'=3.5$ for β-Sn structure, in agreement with $B=86$ GPa reported in a theoretical calculation using the local-density approximation with a nonlinear core-valence interaction.[20] The details of this simulation will be discussed elsewhere.

In the rest of the paper, we will concentrate on the amorphous structure. The pressure-volume curve of a-Ge is given in Fig. 1. The volume changes smoothly up to 12.75 GPa, and at this pressure an abrupt decline of the volume is seen, indicating a first-order phase transition. The volume drops about 19%, which is close to the value of 19.2% obtained in diamond to β-Sn transformation of c-Ge.[17] a-Ge transforms from a low-density amorphous phase to a metallic HDA phase in agreement with the experiment,[5] but the predicted

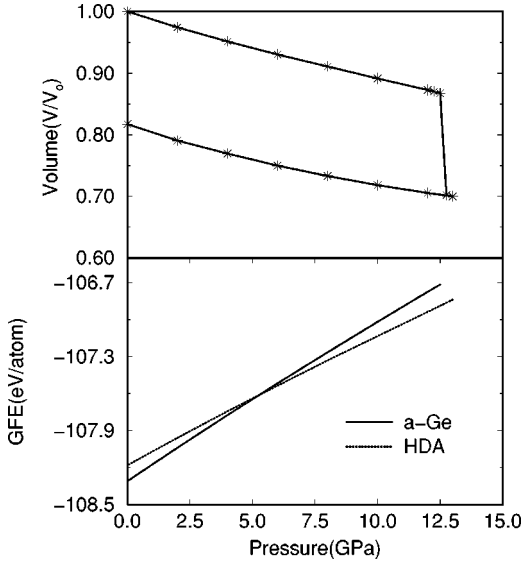

FIG. 1. (a) The pressure dependence of the normalized volume of *a*-Ge. (b) The Gibbs free energy of the amorphous and the HDA phase.

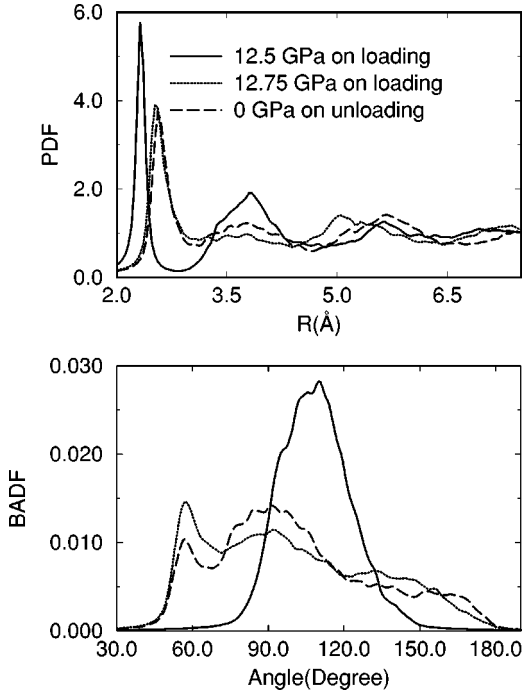

FIG. 2. (a) The real-space pair distribution function. (b) The bond-angle distribution function on compression and decompression.

transition pressure is larger than that of the experiment. The large value of the critical pressure compared to experiments is commonly seen in constant pressure simulations and can be attributed to the kinetics because of the short time scale of the simulation and finite size of the simulation cell. In order to obtain an equilibrium critical pressure, we calculate the Gibbs free energy ($G=E_{tot}+PV$) at zero temperature for *a*-Ge and the HDA phase of Ge. The Gibbs free-energy curve of these phases crosses about 5.2 GPa, which is consistent with the experimental value of 6 GPa.[5] This polyamorphic phase transition is similar to that of H_2O,[1,21] *a*-Si,[2] and SiO_2.[3]

Zero-pressure samples upon decompression are mostly amorphous structure with some crystalline fragments[5,7] and the sample is denser than the initial amorphous structure because of a 5% volume drop at transition pressure.[7] We find that the path on pressure release is not reversed (Fig. 1), and the obtained structure remains amorphous. The structure is found to be 18% denser than the initial amorphous structure indicating an irreversible amorphous to amorphous phase transition as in H_2O,[1,21] *a*-Si,[2] and SiO_2.[3]

The pair distribution function is given in Fig. 2. The positions of the peaks shift gradually to shorter distances, indicating tighter packing of the network, up to the transition pressure at which the first peak shifts abruptly to a larger distance with a broadened distribution and decreased intensity while the third peak continues to move to a shorter distance with a slightly pronounced intensity. However, there is no well-defined second peak at the transition. Upon decompression, the second peak appears gradually and the first and third move to larger distances .

The bond-angle distribution function of *a*-Ge is depicted in Fig. 2. The network exhibits a smooth distribution with a single peak centered at tetrahedral angle up to the transition pressure. At 12.75 GPa, the bond-angle distribution function is rather broad with main peaks around 60°, 90°, and 140°. Upon the pressure release, the height of the peaks at 60° and 90° is reversed, and a relatively similar bond-angle distribution function to that of *l*-Ge is formed even though the density of the high-pressure phase is larger than that of *l*-Ge. The peak at 60° represents a more closed packed structure with typical metallic bonding. Upon decompression, the structure gradually changes from a more closed packed structure to an open structure with some tetrahedral bonding.

The high pressure properties of *a*-Ge are given in Table I. Pressure yields shortened bond lengths and narrowed bond angles up to the transition at which point the average bond angle drops to 98.81° which is intermediate between the tetrahedral and octahedral values of 109.5° and 90° respectively, and the average bond length increases to 2.63 Å. The average coordination from the first minimum of the pair distribution function within a critical cutoff radius $R_c = 3.01$ Å is ~8 and is quite sensitive to choice of the cutoff radius. Upon pressure release, the average bond angle and bond length exhibit a small change, whereas the average co-

TABLE I. Structural properties of *a*-Ge on compression: average bond length (ABL), average bond angle (ABA), width of bond-angle distribution (WBAD), and average coordination number (ACN).

Pressure (GPa)	0	8	10	12.5	12.75
ABL (Å)	2.421	2.357	2.345	2.332	2.638
ABA	109.16°	108.98°	108.90°	108.71°	98.81°
WBAD	10.18	11.09	11.46	12.28	32.37
ACN	4.0	4.0	4.0	4.0	8.03

TABLE II. Structural properties of *a*-Ge on decompression. Same nomenclature as Table I.

Pressure (GPa)	0	2	6	8	10
ABL (Å)	2.667	2.676	2.640	2.639	2.653
ABA	100.73°	100.09°	100.31°	99.97°	99.21°
WBAD	31.30	31.90	31.64	31.92	32.41
ACN	6.48	6.97	6.98	7.27	7.87

ordination is reduced to 6.48 (Table II). This value is close to the coordination of *l*-Ge, 6.8 obtained in an x-ray diffraction study,[22] and 6-7.1 in a first principles calculation.[23] Also the position of the first peak, 2.59 Å , is comparable to 2.70 Å (Ref. 22) and 2.63 Å of *l*-Ge.

The volume change upon compression (up to 12.5 GPa) and decompression can be fitted to the Birch-Murnaghan equation of state.[18] The calculation yields $B=73$ GPa and $B'=3.2$ for *a*-Ge. These values are different from $B=34.5$ GPa and $B'=8$ reported in an x-ray diffraction study,[7] and $B=97\pm8$ GPa and $B'=6\pm2$ obtained in an EXAFS analysis.[8] For the HDA phase, we find $B=55$ GPa and $B'=3.19$. The softening of these bulk modulus compared to the other structures is due to the high coordination, which leads to additional restrictions to the bulk relaxation in the disordered networks.[24]

We can track the electronic nature of the pressure-induced insulator-metal transition in the simulation. With the application of pressure, the valence tail states tend to move toward the center of the band gap. However, the conduction tail states reveal a complex behavior: up to 8 GPa, the states shift to higher energies, producing an increase of the band gap, and after this pressure the states move to lower energies, yielding a decrease of the gap. The response of the conduction tail states to pressure determines the optical gap of *a*-Ge. Simultaneously, a broadening of the band is observed. The Fermi level lies on the middle of the band gap and gradually shifts to a higher energy with an increase of pressure. The pressure dependence of the optical gap is depicted in Fig. 3. The gap *increases* smoothly up to 8 GPa, in agreement with the experiment but, after this pressure it decreases gradually. The band gap exhibits a linear behavior up to 4 GPa and has a slope of 1.68 meV/kbar, which is comparable to the coefficient 0.8 meV/kbar (Ref. 7) and 3.5 meV/kbar.[25] At 12.75 GPa, *a*-Ge transforms to a metallic phase with a sharp drop in the optical gap. The tiny gap is a finite size and minimal basis artifact: the material is certainly conducting.

In order to study the pressure dependence of the localized states, we define the Mulliken charge,[26] $Q(n,E)$, for atom n associated with the eigenvalue E. This charge can then be used as a measure of the localization of a given state $Q_2(E)=N\Sigma_{n=1}^{N}Q(n,E)^2$ where N is the number of atoms in a supercell. For a uniformly extended state, $Q_2(E)$ is 1, while it is N for a state perfectly localized on a single atom. The localization of the electron states near the band gap is depicted in Fig. 3. As expected the states near the band gap are quite localized at zero pressure, and the localization of these states decreases gradually, indicating pressure-induced delocalization of the states, similar to that found in *a*-Si (Ref. 2) and *a*-$GeSe_2$.[14] At the transition pressure the tail states are abruptly delocalized as seen in *a*-Si.

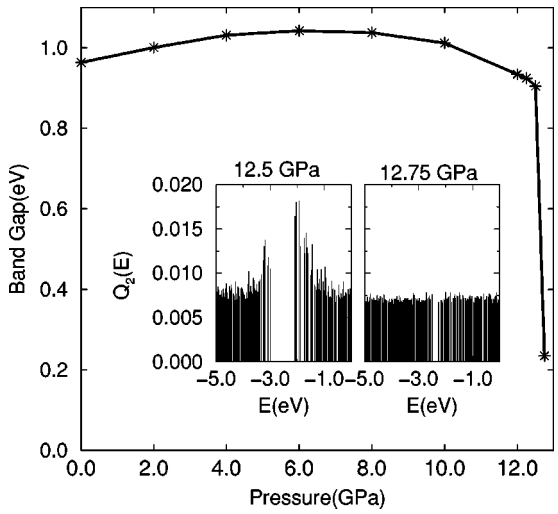

FIG. 3. The pressure dependence of the optical gap. Inset: Electronic eigenstates in the band-gap region. The position of the vertical bars represent the eigenvalues of the electronic eigenstates, and the height of the bars is the spatial localization $Q_2(E)$. The Fermi level lies in the middle of the band gap. Note the abrupt delocalization of the tail states at 12.75 GPa.

It is valuable to predict the pressure dependence of the phonon modes before and after the phase transition. The physical origin of the phase transition can be understood by examining the soft phonon modes. The vibrational density of states (VDOS) is given in Fig. 4. With the application of pressure the acoustic modes soften while the optical band shift to higher frequencies up to the transition pressure, at which point the mode frequencies decline abruptly and the bands overlap as seen in *a*-Si.[2,27] We also find that the localized eigenmodes at zero pressure are extended with pressure. Similar change of localized states has been observed in the theoretical study of *a*-$GeSe_2$,[14] *a*-Si,[27] and SiO_2.[28]

In summary, *a*-Ge undergoes a first-order amorphous to amorphous phase transition, which is due to the ideal amor-

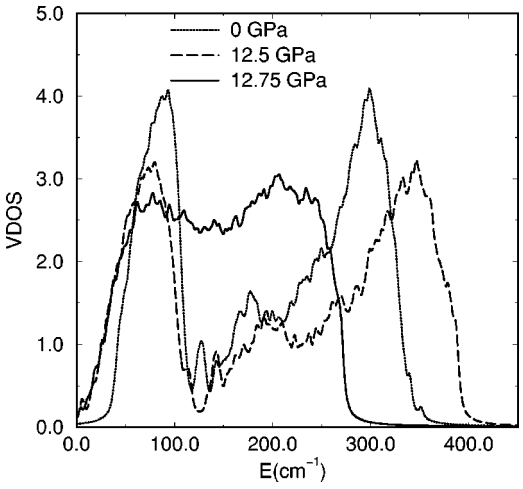

FIG. 4. Vibrational DOS at 0, 12.5, and 12.75 GPa.

phous structure such that no crystalline remnant exists in the network. Nevertheless, it is worth repeating this type of study on large systems with different structures, especially containing crystalline grains, at different temperature.

We would like to thank Professor N. Mousseau for providing us initial amorphous structure. This work is supported by the National Science Foundation under Grant Nos. DMR-00-81006 and DMR-00-74624.

[1] O. Mishima, L.D. Calvert, and W. Whalley, Nature (London) **314**, 76 (1985).
[2] M. Durandurdu and D.A. Drabold, Phys. Rev. B **64**, 014101 (2001).
[3] D.J. Lacks, Phys. Rev. Lett. **84**, 4629 (2000); **80**, 5385 (1998).
[4] G.D. Mukherjee, S.N. Vaidya, and V. Sugandhi, Phys. Rev. Lett. **87**, 195501 (2001).
[5] O. Shimomura, S. Minomura, N. Sakai, K. Asaumi, K. Tamura, J. Fukushima, and H. Endo, Philos. Mag. **29**, 547 (1974).
[6] S. Minomura, *High Pressure and Low-Temperature Physics* (Plenum, New York, 1978), p. 483.
[7] K. Tanaka, Phys. Rev. B **43**, 4302 (1991); J. Non-Cryst. Solids **150**, 44 (1992).
[8] J. Freund, R. Ingalls, and E.E. Crozier, J. Phys. Chem. **94**, 1087 (1990).
[9] P. C. Kelires, CECAM Workshop on Rigidity and Strain Fields in Crystalline and Amorphous Materials, June 25-27, 2001 (Lyon, France), (unpublished).
[10] G.T. Barkema and N. Mousseau, Phys. Rev. B **62**, 4985 (2000).
[11] O.F. Sankey and D.J. Niklewski, Phys. Rev. B **40**, 3979 (1989).
[12] H.S. Chen, and D. Turnbull, J. Appl. Phys. **40**, 4214 (1969).
[13] P. Germain, K. Zellama, S. Squelard, J.C. Bourgoin, and A. Gheorghiu, J. Appl. Phys. **50**, 6986 (1979).
[14] M. Durandurdu, and D.A. Drabold, Phys. Rev. B **65**, 104208 (2002).
[15] M. Durandurdu and D. A. Drabold, Phys. Rev. B. (to be published).
[16] M. Parrinello and A. Rahman, Phys. Rev. Lett. **45**, 1196 (1980).
[17] C. Jamieson, Science **139**, 762 (1963); **139**, 845 (1963).
[18] F. Birch, J. Geophys. Res. **57**, 227 (1952).
[19] H.J. McSkimin, J. Appl. Phys. **24**, 988 (1953); H.J. McSkimin and P. Andreatch, Jr., *ibid.* **34**, 651 (1963); **35**, 2161 (1964).
[20] N. Moll, M. Bockstedle, M. Fuchs, E. Pehlke, and M. Scheffler, Phys. Rev. B **52**, 2550 (1995).
[21] P.H. Poole, U. Essmann, F. Sciortino, and H.E. Stanley, Phys. Rev. E **48**, 4605 (1993).
[22] Y. Waseda, *The Structure of Non-Crystalline Material, Liquids, and Amorphous Solids* (McGraw-Hill, New York, 1980).
[23] R.V. Kulkarni, W.G. Aulbur, and D. Stroud, Phys. Rev. B **55**, 6896 (1997).
[24] V.V. Brazhkin, A.G. Lyapin, V.A. Gonchharova, O.V. Stalgorova, and S.V. Popova, Phys. Rev. B **56**, 990 (1997).
[25] G.A.N. Connell and W. Paul, J. Non-Cryst. Solids **8-10**, 215 (1972).
[26] A. Szabo and N. S. Ostlund, *Modern Quantum Chemistry* (Dover, New York, 1996).
[27] M. Durandurdu and D. A. Drabold (unpublished).
[28] W. Jin, R.K. Kalia, P. Vashishta, and J.P. Rino, Phys. Rev. Lett. **71**, 3146 (1993).